PERGAMON

AE International – Europe

Atmospheric Environment 37 (2003) 4217–4231

ATMOSPHERIC ENVIRONMENT

www.elsevier.com/locate/atmosenv

On the impact of urban surface exchange parameterisations on air quality simulations: the Athens case

Alberto Martilli[a,*], Yves-Alain Roulet[a], Martin Junier[a], Frank Kirchner[a], Mathias W. Rotach[b], Alain Clappier[a]

[a] *Air and Soil Pollution Laboratory, Swiss Federal Institute of Technology, Lausanne (EPFL), 1015-Lausanne, Switzerland*
[b] *Swiss Federal Institute of Technology, Zurich (ETHZ), Institute for Atmospheric and Climate Science, 8057-Zurich, Switzerland*

Received 30 January 2003; accepted 7 July 2003

Abstract

Most of the standard mesoscale models represent the dynamic and thermodynamic surface exchanges in urban areas with the same technique used for rural areas (based on Monin–Obukhov similarity theory and a surface energy budget). However it has been shown that this technique is not able to fully capture the structure of the turbulent layer above a city. Aim of this study is to evaluate the importance for meteorological and air quality simulations, of properly capture the dynamic and thermodynamic surface exchanges in urban areas. Two sets of simulations were performed over the city of Athens (Greece): a first using a mesoscale model with a detailed urban surface exchange parameterisation (able to reproduce the surface exchanges better than the traditional method), and a second with the traditional approach. Meteorological outputs are passed to a Eulerian photochemical model (the photochemical model is run offline). Comparison with measurements shows better agreement for the simulation with the detailed parameterisation. The differences between the simulations concern, mainly, wind speed (maximum difference of 0.5–1 $m\,s^{-1}$), night-time temperatures (2–3°C), turbulence intensity ($2\,m^2\,s^{-2}$) and heat fluxes ($0.15\,K\,m\,s^{-1}$) over the urban area, urban nocturnal land breeze intensity, timing and extension of sea breeze. These differences modify the pollutant distribution (e.g. for ozone maximum differences are of the order of 30 ppb). Differences between the simulations are also found in AOT60 values (inside and outside the city) and in O_3 chemical regimes.

Keywords: Urban boundary layer; Urban surface exchange parameterisation; Mesoscale models; Photochemical models; Coastal air pollution; Sea breezes

1. Introduction

Nowadays, air quality models are widely used to evaluate air pollution abatement strategies (Andersson-Skold and Holmberg, 2000; Metcalfe et al., 2002; Palacios et al., 2002; and many others) and new model output (e.g. accumulated exposure over a threshold, chemical regimes, etc.) are required to estimate the impact of air pollution on human health, vegetation growth and historical buildings preservation. To have this information, the precision in the spatial distribution, as well as the time evolution of pollutant concentrations is crucial. In this context, the modification of the planetary boundary layer (PBL) structure, induced by the presence of an urban area, can play a very important role (Bornstein et al., 1993; Oke, 1995; Martilli, 2002). In the standard version of most of the state-of-the-art mesoscale models, dynamic and thermodynamic surface exchanges in cities are represented using the same formulations adopted in rural areas (mainly based on

*Corresponding author. Department of Earth and Ocean Science, University of British Columbia, 6339 Stores Road, Vancouver, BC, Canada V6T 1Z4. Tel.: +1-604-8220531; fax: +1-604-8226088.

E-mail address: amartilli@eos.ubc.ca (A. Martilli).

1352-2310/$ - see front matter
doi:10.1016/S1352-2310(03)00564-8

the constant flux-layer assumption of the Monin–Obukhov similarity theory, and a surface energy budget) adapting the roughness length and the soil thermal capacity. However series of field measurements (Rotach, 2001) have shown that the constant flux layer assumption is not valid in the so-called urban roughness sublayer (from street level up to 2–3 times the mean building height). Consequently, the standard approach is not able to reproduce the vertical structure of the turbulent fields in this layer. Furthermore, in standard mesoscale models, the surface temperature is computed from a surface energy balance that does not take into account shadowing and radiation trapping effects in street canyons, which are one of the phenomena responsible of the urban heat island.

The question that arises is: how does this lack of precision affect the simulated air pollutant distribution? Or, in other words, how precise and detailed an urban surface exchange parameterisation must be to accurately simulate dispersion of primary and secondary pollutants? To attempt to answer these questions a series of numerical simulations for Athens (Greece), a polluted city in complex terrain, have been performed with a system composed by a numerical mesoscale model and an Eulerian photochemical model. Two simulations are carried out: one with a detailed urban surface exchange parameterisation (Martilli et al., 2002; in the following this simulation will be labelled *urban*), and the second with the traditional and less detailed approach used in mesoscale models to represent urban surfaces (modification of the roughness length and the soil thermal capacity, in the following will be called *trad*). The meteorological parameters are then, independently, used as input for an Eulerian photochemical model, which computes pollutant dispersion and chemical reactions. The comparison between the results of the two simulations will give some clue to understand the effect on air pollution of properly capturing the dynamic and thermodynamic influences of the urban surface on the atmosphere in which the pollution is occurring.

2. Simulations

2.1. Mesoscale model

The mesoscale numerical model used is non-hydrostatic, Boussinesq, and anelastic (Clappier et al., 1996; Martilli et al., 2002). The mean transport is computed with a third-order parabolic piecewise method (PPM, Collella and Woodward, 1984) corrected for multi-dimensional applications (Clappier, 1998). In the transition layer, turbulent coefficients are derived from turbulent kinetic energy (TKE, computed prognostically), and a length scale, following the formulation of Bougeault and Lacarrere (1989). In the surface layer (corresponding to the lowest numerical level), in rural areas, the formulation of Louis (1979) is used. The ground temperature and moisture, in rural areas, are estimated with the soil module of Tremback and Kessler (1985).

The urban parameterisation of Martilli et al. (2002) represents the city as a series of parallelepiped of concrete of uniform width and spacing, but with different heights. The lowest model level is at the physical ground and several grid levels are within the urban canopy. The main differences between this formulation and the traditional approach of modifying the roughness length and the soil thermal characteristics are:

- The impact of the presence of the buildings on the airflow (momentum sink, TKE production, heat fluxes) is vertically distributed among all levels within the canopy, and not only at the ground. As a consequence the Reynolds stress increases (in magnitude) with height in the canopy (in agreement with urban measurements (Rotach, 1993a)).
- The modification on the length scales limits the increase of TKE in the canopy (again in agreement with several urban measurements (Rotach, 1993b; Louka et al., 2000) and wind tunnel studies (Kastner-Klein et al., 2001)).
- The trapping of radiation and shadowing effects in the urban canyons are taken into account. Due to this mechanism, for example, it is possible to reproduce the nocturnal urban heat island effect, while with the traditional approach it is not.

In both parameterisations, the latent heat fluxes are neglected. Unfortunately, to the knowledge of the authors, there are no urban latent heat fluxes measurements for the period studied. However, measurements taken in other densely urbanized areas (downtown Vancouver and Mexico city) show extremely small latent heat fluxes (Grimmond and Oke, 2002), making the approximation not completely unrealistic. Moreover, Grimmond and Oke (2002) found that the most important source of latent heat fluxes in urban areas is irrigated parks and gardens. So neglecting the latent heat fluxes in urban areas corresponds to neglecting the effect of parks and gardens. As it can be seen from a satellite picture of Athens, with the exception of a small area around the Acropolis this assumption is quite realistic for the city of Athens.

2.2. Air quality model

The transport and photochemistry Eulerian model (TAPOM) was developed at the Swiss Federal Institute of Technology, Lausanne (EPFL), and at the Joint

Research Centre of Ispra (JRC-Ispra) to simulate photochemical air pollution. It includes the RACM lumped species mechanism (Stockwell et al., 1997), the Gong and Cho (1993) chemical solver, an improved highly accurate transport algorithm (Collella and Woodward, 1984; Clappier, 1998) and the solar radiation module TUV developed by Madronich (1998) to calculate the photolysis rate constants.

2.3. Case study, numerical domain, initial and boundary conditions

The city of Athens (Greece) is chosen as case study. Athens is a very polluted city (Moussiopoulos, 1994), because of a high population density (four million inhabitants in an area of about 500 km^2), and also because recirculation processes, linked with the land–sea breeze cycle, enhance air pollution levels. When the synoptic forcing is low, photochemical smog episodes frequently occur. Several modelling studies have already been done for this area (e.g., Moussiopoulos et al., 1995; Clappier et al., 2000). Here, the case of the 14 September 1994, when the MEDiterranean CAmpaign of PHOtochemical Tracers-TRAnsport and Chemical Evolution (MEDCAPHOT-TRACE) experimental campaign took place, is considered. For this day a large set of meteorological measurements (air temperature, wind speed and direction, etc.) and pollutant concentrations is available.

The domain (72 km × 72 km) encompasses the Saronic Gulf and Aigina Island to the south, Mt. Parnitha to the North, Pendeli and the Hymettus Mountains to the East (Fig. 1). The city is located in the basin surrounded by Parnitha, Pendeli and Hymettus Mountains. In the city two areas can be distinguished (Fig. 1): the downtown area covering an area of 72 km^2 (1.4% of the domain) and the suburban region covering an area of 328 km^2 (6.3%). The rest of the land is rural (49.3%). The sea occupies 43% of the domain.

The horizontal resolution is 2 km × 2 km, resulting in 36 grid points for each side. At the lateral boundaries, eight additional grid cells with spacing ranging from 2.4 to 8.7 km (grid stretching ratio equal to 1.2) are used to move boundaries away from the domain of interest to reduce their influence on the flow. These additional cells lead to a total dimension of 151 km × 151 km for the domain used for the dynamics. The vertical resolution is 10 m for the lowest five levels, and then it is stretched up to the top of the domain at 8500 m (maximum spacing 1000 m). Domains of similar size and resolution have

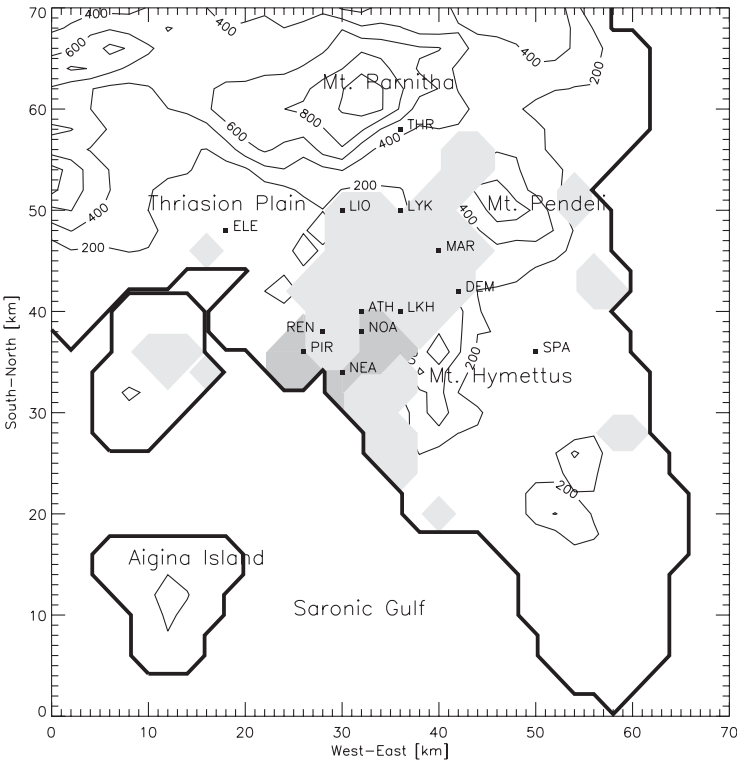

Fig. 1. The simulation domain. The suburban area is light grey, and the downtown area is dark grey. The measurements stations are: National Observatory of Athens (NOA), Marousi (MAR), Elefsis (ELE), Thrakomakedones (THR), Rentis (REN), Lykabettus Hill (LKH), Liosia (LIO), Demokritos (DEM), Athinas Street (ATH), Pireaus (PIR), Nea Smirni (NEA), Lykobrisi (LYK), Spata (SPA).

been used already in the past in other studies (Clappier et al., 2000; Varvayanni et al., 1998; Moussiopoulos et al., 1997).

Detailed data regarding the morphology of the city were not available. In agreement with the measurements taken by Ratti et al. (2001) for other European cities, downtown is represented by an average building height of 20 m (equivalent to approximately 6–7 storeys resulting from the following distribution: 10% of the buildings 10 m, 25% 15 m, 30% 20 m, 25% 25 m, and 10% 30 m), while in the suburban area buildings have an average building height of 10 m (3 storeys with 20% of the buildings 5 m high, 60% 10 m, and 20% 15 m). The street width is 10 m as well as the horizontal building size (resulting in a built up to total area ratio of 0.5, in the range measured by Ratti et al., 2001). For both classes (suburban and downtown) two street directions are defined: 45° from North (perpendicular to the coast in the area of the city) and 135° (as it can be seen in a city map, these are the two most common directions in the area). Assuming this morphology, the roughness for the *trad* simulation is set to 1 m for the suburban area and to 2 m for downtown (following the rule of thumb given by Grimmond and Oke, 2000). The thermal properties of the buildings are in Table 1 (for the *trad* simulation the thermal properties are those of the floor).

In the rural area, soil type is sandy-clay-loam (Trembback and Kessler, 1985) and initial soil moisture content is 0.21 (volume of water per volume of soil). Simulations start at 2000 LT and last for 28 h (the first 4 h are considered a spin-up period and are not used in the analysis). The initial wind (derived from a sounding at Hellenikon airport and used also as geostrophic) is weak (1 m s^{-1} in the lowest 3000 m and 2 m s^{-1} aloft) and from northwest (340°). The initial atmospheric stability is 3.5 K km^{-1} (initial potential temperature at ground is 300 K). The sea surface temperature is 296 K. The synoptic conditions of the simulated day are typical for summer periods in the region. The weather conditions over eastern Greece and the Aegean Sea are the result of a balance between a high-pressure system over the eastern Mediterranean and the Balkans up to the Black Sea, and a thermal low pressure over the Anatolian Plateau (southeast of the Balkans and the Black Sea) due to ground heating (Kallos et al., 1993). When the high-pressure system strengthens, it extends westward and the pressure gradient across the Aegean Sea weakens. Consequently, the northerly synoptic wind over the Athens basin becomes weaker and a local, thermal sea–land-breeze circulation develops (this was the situation of 14 September 1994).

Boundary conditions for photochemical simulations, based on air-flight measurements recorded on 12 September (no aircraft data are available for the 14th), are 60 ppb of O_3 and 0.01 ppb of NO and NO_2 (the same conditions used by Clappier et al., 2000). The emissions (corresponding to the early 1990s) are a combination of two inventories: the data described in Ziomas and Coauthors (1995) are used for the harbour, the industry and the extra-urban traffic, and the car traffic emission in the city centre is taken from Arvanitis et al. (1997) and Moussioupoulos et al. (1997). The temporal resolution of the emission is 1 h, while the spatial resolution is 2 km × 2 km. Biogenic emissions are not taken into account, therefore there is no dependence on meteorology (this is the same emission inventory used by Clappier et al., 2000). A pre-run of 1 day, with the same emissions and the same wind field starting from a constant background equal to the boundary conditions values was performed to provide more realistic initial conditions for the simulation.

3. Meteorological results

3.1. Comparison with measurements

Measured nocturnal temperatures (Fig. 2) are around 23–24°C for suburban stations (Liosia, Marousi, Demokritos, Fig. 1) and even higher in the downtown area (Peireaus, NOA), but they drop to 15–16°C in the rural area (Spata), showing a strong nocturnal urban heat island of 8–10°C. During daytime, as expected, differences are much smaller, with a maximum temperature in the urban area of about 31–32°C and 30–31°C for the countryside. The largest differences between the two simulations occur at night for the stations located in the suburban and downtown areas. At the suburban

Table 1
Parameters used in the urban module

Surface	K_s (e−06 $m^2 s^{-1}$)	C_s (e–06 J $m^{-3} K^{-1}$)	T (int) (°C)	ε	α	z_0(m)
Wall	0.67	1	20	0.90	0.2	
Roof	0.67	1	20	0.90	0.2	0.01
Floor	0.286	1.4	17	0.95	0.2	0.01

K_s is the substrate thermal conductivity of the material, C_s is the specific heat of the material, T (int) is the initial temperature of the material and also temperature of the deepest layer, ε is the emissivity of the surface, α is the albedo of the surface and z_0 is the

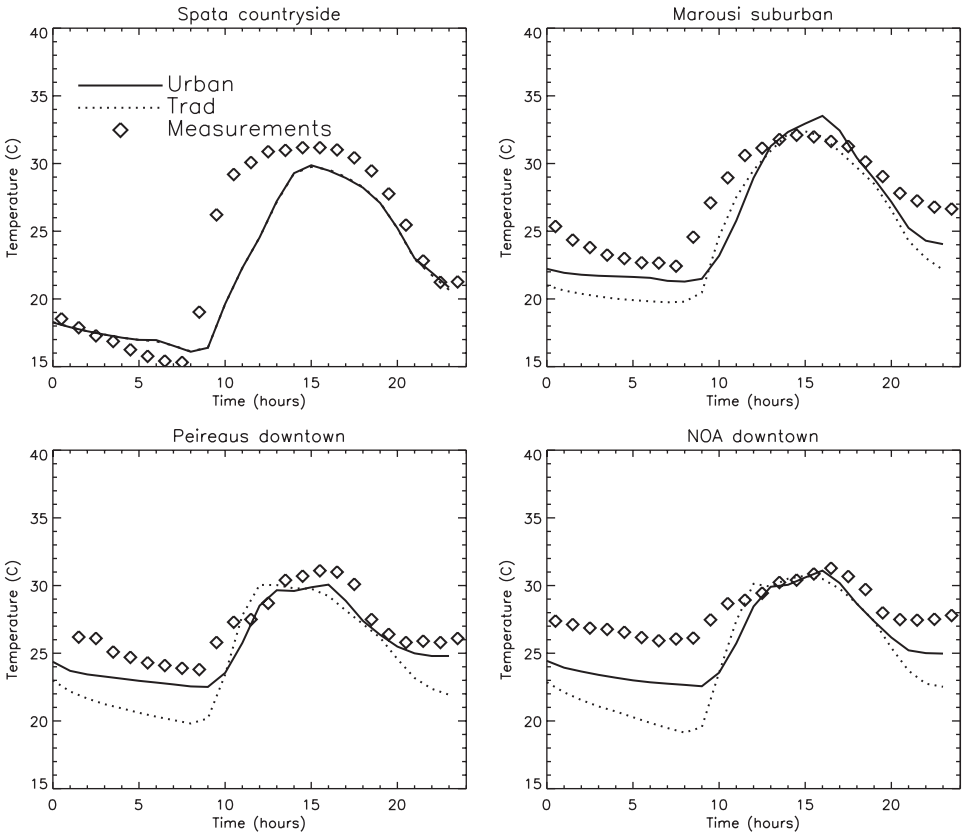

Fig. 2. Time series of air temperature at 10 m AGL for different stations for 14 September 1994.

stations, temperatures of *urban* are in better agreement with measurements and 1.5–2°C higher than *trad*. Slightly larger differences are found for downtown stations, but here *urban* underestimates measurements by around 2°C. In the countryside, the two simulations are close (as expected) and they overestimate measurements by around 2°C during night. During daytime, *urban* and *trad* reproduce quite well the maximum.

The station of Elefsis, located in the countryside in the Thriasion Plain (northwest of the domain), experienced very weak winds during the night (less than $1\,m\,s^{-1}$), and southerly winds ($2–3\,m\,s^{-1}$) during daytime in correspondence with the sea breeze development (Fig. 3). Both simulations are able to reproduce the southerly wind during daytime, but with an overestimation of the speed. At this countryside location the differences between *urban* and *trad* are very small.

Suburban stations of Marousi and Demokritos (Fig. 3), located in the northeastern part of the city, experienced, also, wind speed of $1\,m\,s^{-1}$ or less during night increasing up to $2–3\,m\,s^{-1}$ during day. At Marousi, during day, the wind turns progressively from northwest to southeast. This rotation is induced by the afternoon penetration of the sea breeze developed over the Eastern part of the peninsula through the gap between Mounts Pendeli and Hymettus, as confirmed by the measurements at Demokritos station, located on this gap, showing a sudden change of direction at around 1400 LT from West to southeast. This behaviour is in general quite well reproduced by the simulations but at different times (the rotation of the wind speed happened earlier in *trad*, then in *urban*). Wind speed is also relatively well captured by both simulations.

In the downtown area (Fig. 4), weak winds from North are measured during night, while during daytime a Southerly sea breeze develops ($1.5–2\,m\,s^{-1}$ slightly weaker than in the suburban area). Both simulations captured the direction, while the intensity is slightly overestimated by *trad* at Peireaus and Nea Smirni and better reproduced by *urban*. Finally, the NOA station measured higher wind speed ($1.5–2\,m\,s^{-1}$ during night and $4–4.5\,m\,s^{-1}$ during day) than the other two downtown sites and both simulations underestimate it (especially during daytime). It must be emphasized, however, that this station was located in a park on a small hill (Batchvarova and Gryning, 1998), not resolved by the model, which has a horizontal resolution of $2\,km \times 2\,km$.

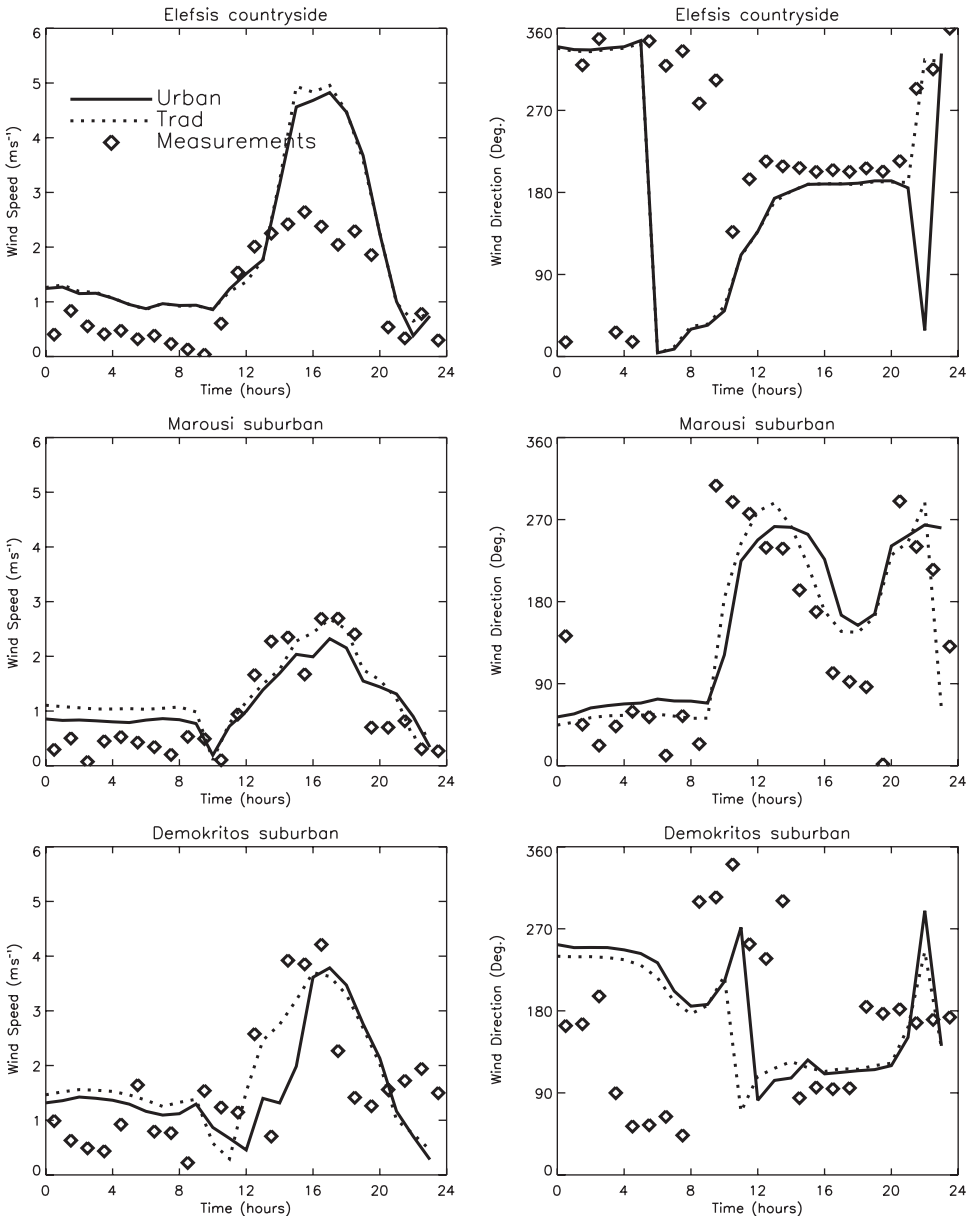

Fig. 3. Time series of wind speed and direction at 10 m AGL for rural and suburban stations for 14 September 1994.

At the suburban station of Marousi, some turbulence measurements recorded at 15 m above ground level are also available. The measured TKE (Fig. 5a) is quite low during night time, as expected, and increases up to $1.5\,m^2\,s^{-2}$ during daytime. The *trad* simulation has very strong turbulence ($4\,m^2\,s^{-2}$) during day, while *urban* has lower values, closer to the measurements (maximum of $1.7\,m^2\,s^{-2}$). Moreover, the rate of increase of TKE in the morning is larger in *trad* than in *urban*. A similar behaviour can also be found for the sensible heat fluxes (Fig. 5b). For this variable, model results are higher than measurements during daytime (and a possible explanation of this difference can be in the fact that both simulations neglect the latent heat fluxes). However, it must be kept in mind that fluxes were measured within the urban roughness sublayer, a region where turbulent fluxes have a strong vertical gradient. As it is shown in Fig. 5c, the vertical profile of TKE during daytime computed by *trad* shows a strong increase near the ground, while *urban* has a slower increase in the urban canopy. Moreover also the vertical profile of sensible heat flux (Fig. 5d) has a different structure in the two

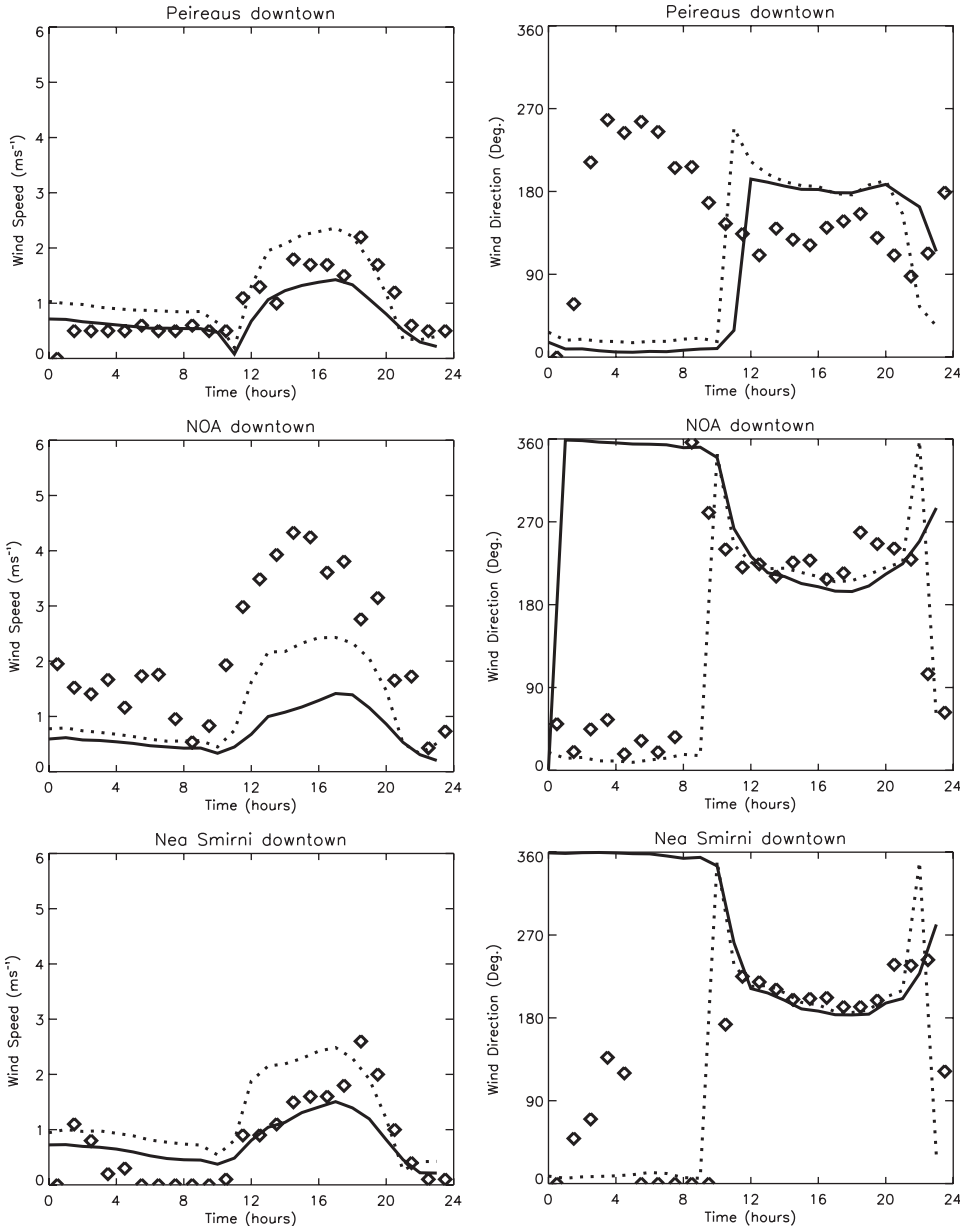

Fig. 4. Time series of wind speed and direction at 10 m AGL for downtown stations for 14 September 1994 (symbols are the same as Fig. 3).

simulations (near constant in *trad* as prescribed by the surface layer theory, which does not hold in the roughness sublayer, and increasing with height for *urban*).

In the interpretation of the differences between the simulations the following points must be considered:

- The *urban* module stores more energy (during daytime) than the *traditional* one (Martilli et al., 2002). Since in both cases latent heat fluxes are neglected, this explain why the sensible heat fluxes (and, as a consequence, the generation of TKE by buoyancy effects) are lower in *urban*.
- The modification of the turbulent length scales (in *urban*) act to reduce the TKE within and just above the canopy.

Moreover, during nighttime the heat flux is near to zero in the measurements and in *urban*, while in *trad* it is negative. This means that the cooling is smaller in *urban*

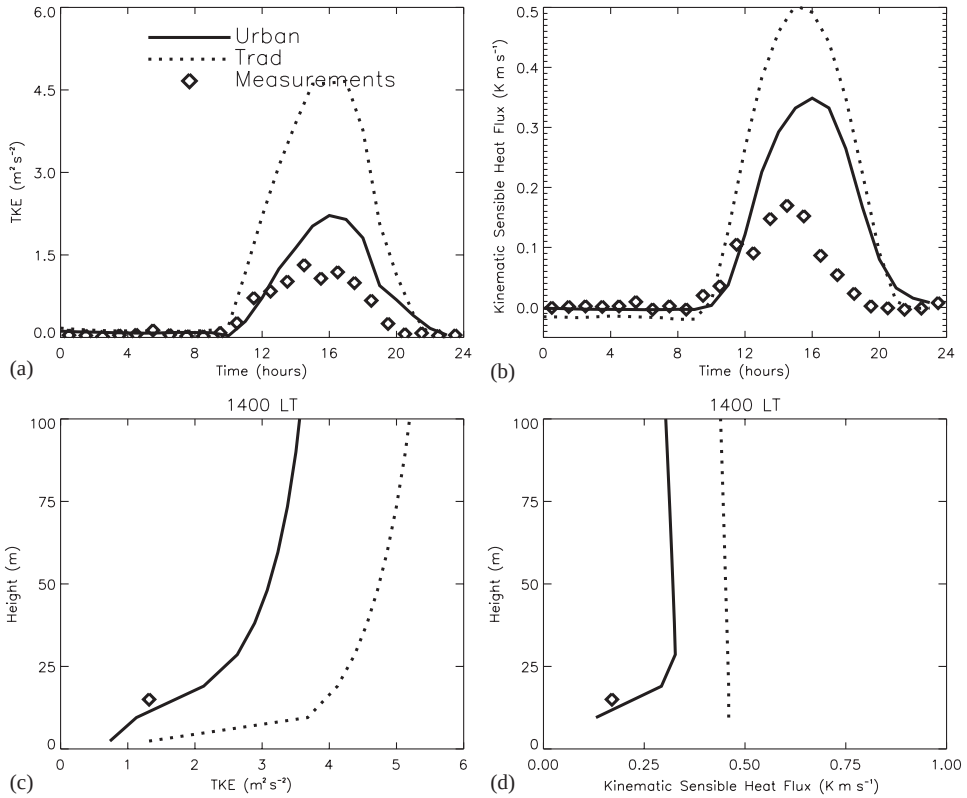

Fig. 5. Time series of (a) TKE and (b) kinematic sensible heat flux at 15 m AGL and vertical profiles at 1400 LT for (c) TKE and (d) kinematic sensible heat flux for Marousi for 14 September 1994.

than in *trad* and it explains the higher temperatures computed during night (Fig. 2).

3.2. Wind fields

Nocturnal flow fields (Fig. 6a) are characterised by slope winds on the principal topography of the domain, land breezes and a weak, northerly wind in the region of the city. *Trad* (differences relative to *urban* in Fig. 6b) generates weak winds (similar to *urban*) over Athens, while over the sea a stronger land breeze develops (this is due, again, to the fact that temperatures in the city are colder in *trad* than in *urban*, see Fig. 2).

During daytime (1400 LT) the situation changes. In *urban* (Fig. 6c), the sea breeze is well developed on both sides of the peninsula, and the convergence zone is located on Mounts Hymettus and Pendeli. Weak winds are computed in the region of the city. North of the city and just South of the Parnitha Mountain, *trad* shows a rotation of the wind direction from West with respect to *urban*, which has more southerly wind (Fig. 6d). The reason for this difference is probably due to the higher sensible heat fluxes simulated by *trad* as compared to *urban* in the city (see Fig. 5b at Marousi). This induces a higher temperature gradient between the city and the countryside, resulting in a stronger pressure gradient deviating the wind towards the city. For the same reason (difference in the sensible heat fluxes) in the gap between Mount Pendeli and Mount Hymettus, the sea breeze coming from the Eastern part of the peninsula penetrates 3–4 km more in *trad* than in *urban*.

In conclusion, the most important meteorological differences between the two simulations are:

- In the city, nocturnal temperatures are higher and closer to the measurements in *urban* than in *trad* (nocturnal urban heat island effect, also induced by the fact that *urban* takes into account the trapping of radiation in the urban canyon, but *trad* not). As a consequence, land breezes over the sea are stronger in *trad* than in *urban*.
- During daytime, both simulations reproduce sea breeze as observed in the measurements, but in the downtown region, *trad* slightly overestimates wind speeds, while *urban* has a better agreement.
- Surface sensible heat fluxes in the region of the city are smaller, and closer to measurements in *urban* than in *trad*. Moreover, the temperature gradient between the countryside and the city is stronger in

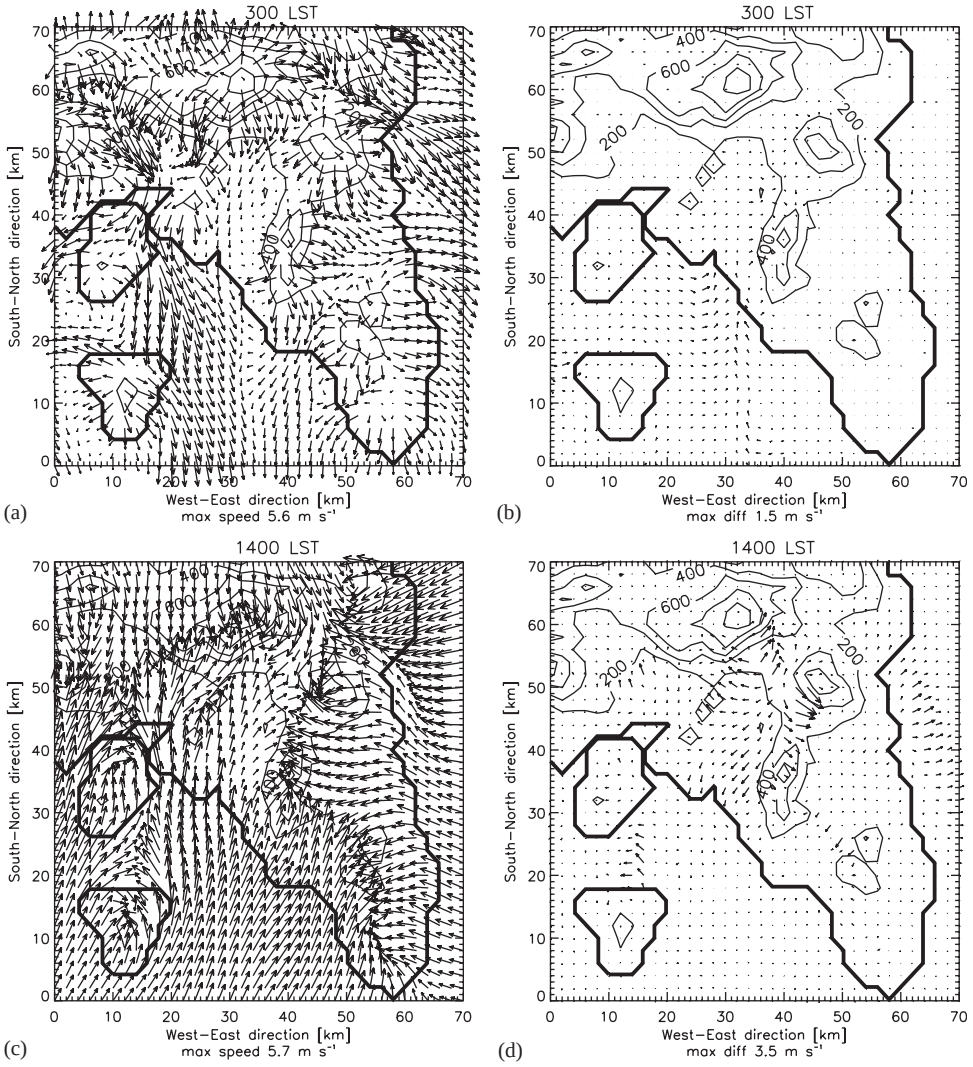

Fig. 6. (a) Wind field at the lowest model level (5 m) for the *urban* simulation at 0300 LT 14 September 1994. (b) Vector difference between the wind field of the *urban* and the *trad* simulations at the same hour. (c) Wind field at the lowest model level for the *urban* simulation at 1400 LT of the same day. (d) Vector difference between the wind field of the *urban* and the *trad* simulations at the same hour.

trad, and this modifies the position of the sea breeze convergence.

4. Chemical simulations

4.1. Comparison with measurements

Athina Street, Marousi, Liosia, Rentis and Lykobrisi are in a region of very high emissions (Fig. 7). The measured NO_x mixing ratios are high during night, peak in the morning hours (increase in traffic) and are low during the day, when the strong turbulent activity disperses pollutants. The two simulations reproduce this behaviour with some discrepancies when compared to the observed data. In particular, at Marousi, and Athina Street, *urban* has a morning peak higher than *trad* and in better agreement with the observations. This is probably linked to the different rate of increase of TKE in the morning in the two simulations (Fig. 5), as well as with the reduction in TKE in the urban canopy induced by the modifications in the length scales. On the other hand, at Liosia, close to the northwest boundary of the city, both simulations overestimate the peak, but with opposite, behaviour (higher peak for *trad* and lower for *urban*). For these stations during daytime *urban* reproduces higher values, in quite good agreement with measurements. Both simulations overestimate NO_x

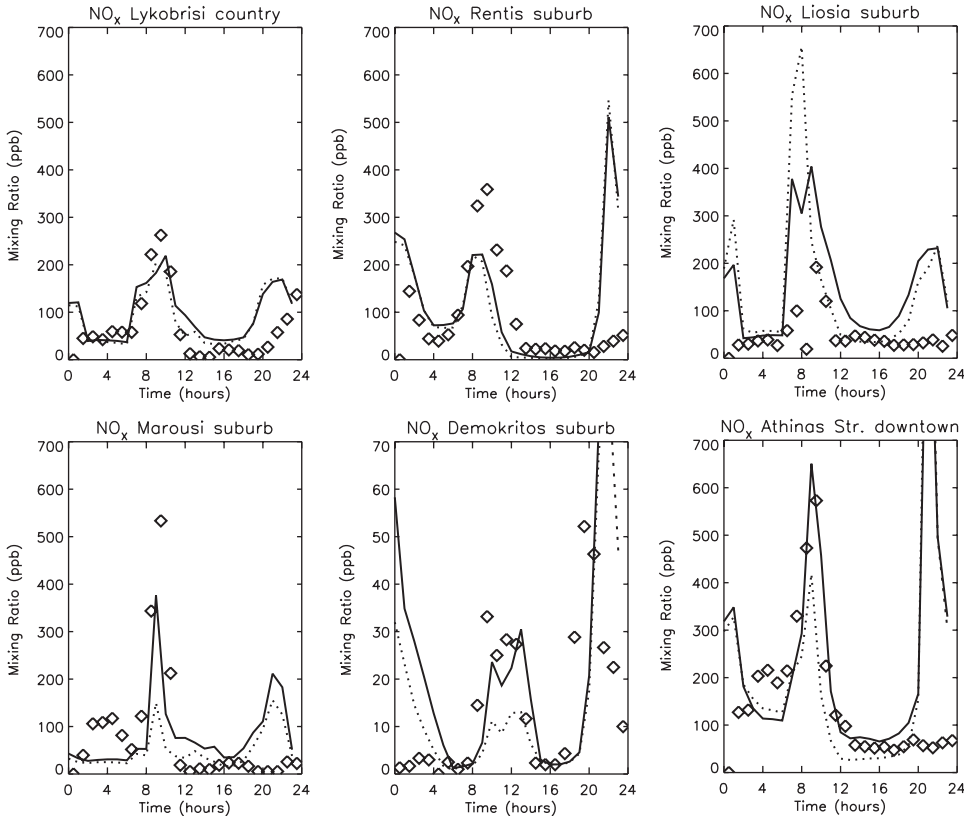

Fig. 7. Time series of NO_x mixing ratio for different stations (note that for Demokritos the vertical scale is different) for 14 September 1994 (symbols are the same as Fig. 3).

levels at evening in the city, in particular for downtown (this is probably linked to a too fast decrease in mixing height and an underestimation of wind speed). The situation is different for Demokritos, located outside the region of strong emissions, where lower concentrations were measured. At this station values are low during nighttime, but increase between 1000 LT and 1400 LT, in response to the sea breeze arrival from the Athens basin. This peak is quite well reproduced by *urban*, while *trad* underestimates it.

The highest O_3 mixing ratios (140–150 ppb) were measured at Lykabettus Hill, Demokritos, Marousi and Thrakomakedones, located on a line from Mt. Hymettus to Mt. Parnitha (Fig. 1), close to the sea breeze front at 1400 LT (Fig. 6). Moreover, elevated mixing ratios (greater than 100 ppb) were recorded, also, at Lykobrisi, and Liosia, located in the Northern and Eastern part of the city. Both simulations show elevated O_3 levels at the same locations (Fig. 8), meaning that the position of the O_3 plume is well reproduced. Differences in peak intensity are mainly in the Northern part of the city, (Marousi, Demokritos, Thrakomakedones and Lykobrisi), where *urban* has a peak 15–20 ppb higher than *trad*, and closer to the measurements, except for Lykobrisi. This is probably linked to the higher sensible heat fluxes generated by *trad*, resulting in a higher PBL and to the time of penetration of less polluted air masses from the Spata basin. Finally, at stations located downtown (Athinas Street), in the Western part of the city (Rentis), or in the countryside West of the city (Elefsis), lower values of O_3 (60–80 ppb during daytime) were measured. Models reproduce them for Elefsis, but for the other stations *urban* has a peak of around 100–110 ppb, while slightly lower values (80–100 ppb) are estimated by *trad*, meaning that the elevated O_3 region computed by the models is larger than what was observed on 14 September 1994.

4.2. Pollutant spatial distribution

In this section, the differences between the three simulations in the spatial distribution of the pollutants are analysed over the entire domain. During night, primary pollutants like NO_x or VOC are trapped in a shallow boundary layer over the city and pushed south over the sea, by the land breezes. In the same region O_3 is destroyed by the reaction with NO. *Trad* shows less NO_x in the city and more over the sea, due to the

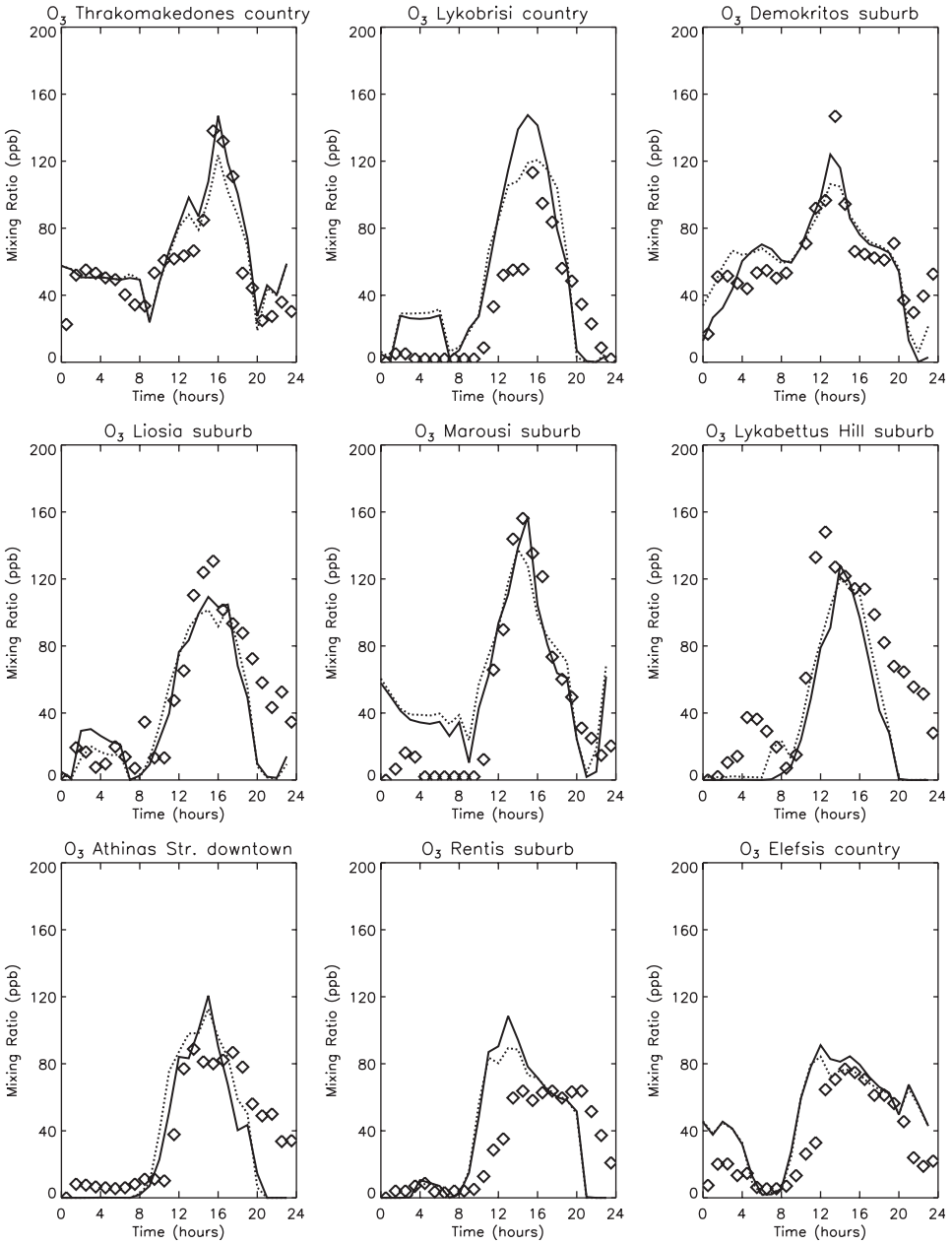

Fig. 8. Time series of O_3 mixing ratio for different stations for 14 September 1994 (symbols are the same as Fig. 3).

differences in wind fields (stronger land breeze over the sea, Fig. 7c).

During daytime (1400 LT) sea breeze is well developed over the peninsula (Fig. 6) and two O_3 maxima are computed (Fig. 9a): one over the sea, due to the photochemical transformation of the pollutants emitted during the previous night and stored over the sea, and one northeast of the city, close to the sea breeze front (in the same region where O_3 maxima were measured, see above). Since sea breezes are stronger for *trad* (Fig. 6) pollutants are transported quicker from the sea to the land. For this reason over the sea, O_3 levels are lower in *trad* than in *urban*, with maximum differences of the order of 35 ppb (Fig. 9b). As already seen in Fig. 8, *trad* has lower O_3 also over the land (maximum differences of the order of 25 ppb).

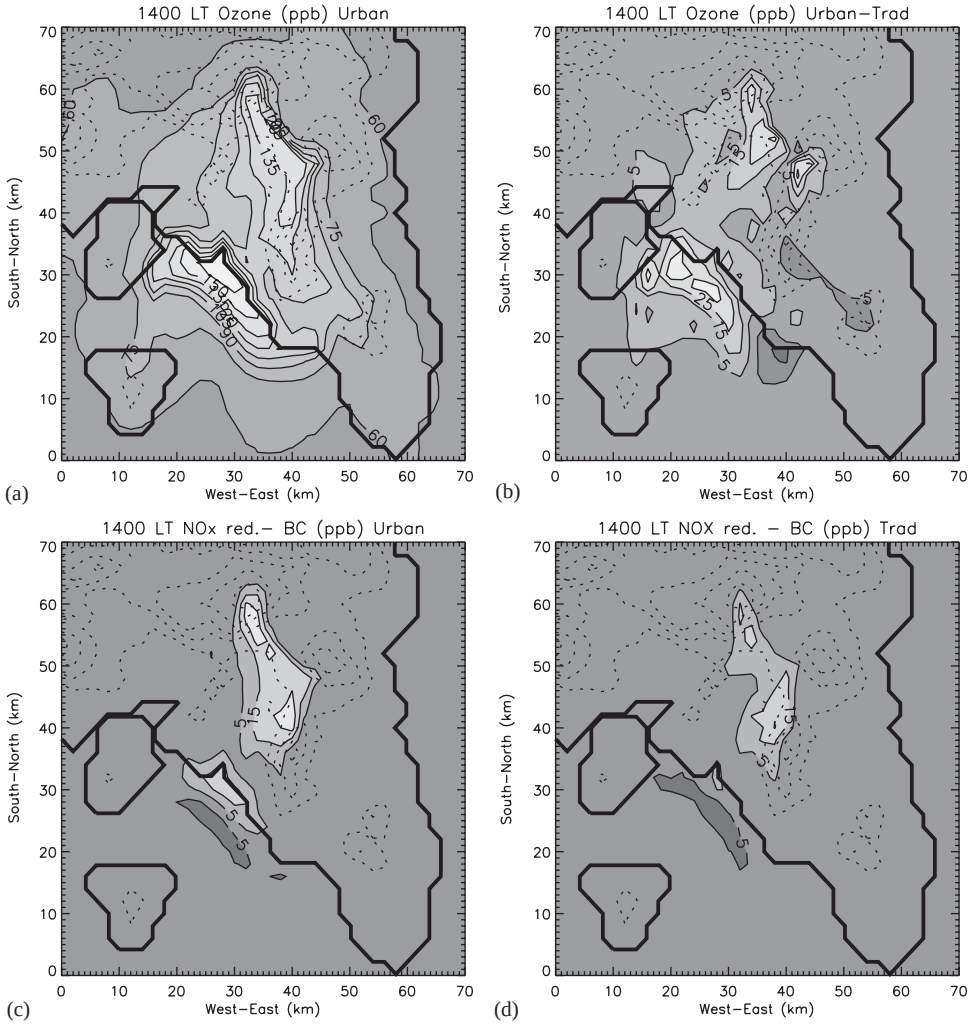

Fig. 9. (a) Map of O_3 (ppb) modelled by *urban* at the lowest model level (5 m) at 1400 LT 14 September. Isolines are every 15 ppb. (b) Difference between O_3 (ppb) modelled by *urban* and *trad* at the same hour and same level. (c) Map of O_3 (ppb) differences between *urban* base cases (100% of emissions) and *urban* case with NO_x emissions reduced by 25%, at the same hour. (d) Same but for *trad*.

5. Impact on the peak, AOT 60 values, and chemical regimes

Two of the most frequently used parameters to evaluate the impact of air pollution on human health or vegetation growth are the peak and the AOT 60 (the integral over time of pollutants mixing ratio above a certain threshold, in this case 60 ppb). In this section, the differences between the two simulations for these parameters are analysed for four different regions distinguished by the land use (sea, countryside, suburban area and downtown).

Values for O_3 are in Table 2. The AOT60 is the average for all the points with the same land use. For the countryside only the region of the photochemical smog is considered (points where the mixing ratios have exceeded 90 ppb at least once in at least one of the simulations). Over all the regions, *urban* has higher O_3 peak. For the AOT60, *urban* computes higher values, because of the larger extent of the O_3 cloud. Results for the sea and the countryside region show that the method used to represent the urban areas has an impact also outside the city.

To analyse the impact of the urban surface scheme on a pollutant with a different chemical behaviour, the same methodology has been used for NO_2 (Table 2). In this case, over the sea higher NO_2 peak and AOT60 are computed by *trad* (as explained above, land breezes are stronger in the trad case, and more pollutants are transported over the sea during nighttime as compared to *urban*). However over the city (suburban and downtown), since the peak of NO_2 is strongly linked with the

Table 2
Peak and AOT60 values for O_3 and NO_2 for every landuse category and for the different simulations

	Peak (ppb)				AOT 60 (ppb h)			
	Sea	Country	Suburb	Downtown	Sea	Country	Suburb	Downtown
O_3								
Urban	176	163	163	131	85	208	216	195
Trad	162	143	149	123	76	196	207	199
NO_2								
Urban	134	225	368	308	30	158	346	831
Trad	164	238	339	245	62	148	258	634

AOT60 values are the average over all the points with the same landuse. For the countryside, only the points where at least one of the two simulations computed at least once more than 90 ppb are considered in the computation of the AOT60.

rate of increase of TKE in the morning *urban* has higher values than *trad*.

Since numerical simulations are very often used to understand which is the best abatement strategy, it is important to analyse the chemical regimes (sensitivity of O_3 levels to a change in NO_x and VOC emissions). For every configuration two more simulations are performed, one with a reduction in NO_x emissions of 25% and another with a reduction in VOC emissions of 25%. For *urban*, a reduction in NO_x emissions increases O_3 levels by a maximum of 30 ppb over land (Fig. 9c), meaning that the chemical regime is NO_x saturated. In the same region a reduction in VOC emissions reduces O_3 levels by a maximum of 33 ppb (not shown). The region of the second O_3 maximum, over the sea, is split in two parts: the southern part is NO_x limited, while the northern part is NO_x saturated. In *trad*, the NO_x saturated region over the land is less intense (25 ppb maximum difference, Fig. 9d) and smaller (192 km^2) than the corresponding region in *urban* (276 km^2). Moreover, over the sea, there is only a NO_x limited region. These results show that the method used to represent the city in a numerical simulation can have an impact on the diagnosed chemical regimes and on the spatial extensions of the NO_x limited and NO_x saturated regions.

6. Conclusions

In this study two mesoscale numerical simulations are performed over the Athens area: one with a detailed urban parameterisation for the city (*urban*), and a second with a simple urban parameterisation (*trad*, modification of the roughness length and the soil characteristics, the traditional method employed in standard mesoscale to represent a city). Meteorological parameters are then used to drive two air quality simulations using an Eulerian photochemical model. Results are compared to meteorological and pollutant measurements.

The *urban* simulation exhibits a generally better skill in predicting suburban and downtown surface temperatures, wind speed, TKE. Sensible heat flux is overestimated by both simulations during daytime and only the *urban* simulation is able to reproduce the near zero heat flux during the night. Both simulations reproduce high O_3 in the same region where the highest levels were recorded. Some differences are in the peak intensity, with a tendency to underestimate it for the *trad* simulation. The morning peak of NO_x is better reproduced by *urban*, while both simulations overestimate the NO_x levels in the evening. Moreover, the methodology used to treat surface fluxes in urban areas has an impact on mesoscale circulations (in this case, land/sea breeze intensity). As a consequence, primary and secondary pollutant distributions, and parameters linked, like AOT60 and chemical regimes, are also affected.

Finally, it must be stressed that these results are relative to the situation of the city of Athens and they should be considered as an example for the case of a city in very complex terrain. The intensity of the modifications induced by the difference in surface sensible heat fluxes (mainly during daytime) between the city and the countryside can change for other locations, situations or seasons of the year. Furthermore, the characteristics of the city itself can reduce or enhance the differences between the detailed urban parameterisation and the simpler one.

Acknowledgements

The authors thank Prof. Douw G. Steyn for suggestions in the preparation of the manuscript, and the bid committee for the "Athens 2004" Olympics for the

emissions inventory. This work has been funded by ERCOFTAC.

References

Andersson-Skold, Y., Holmberg, L., 2000. Photochemical ozone creation potentials (POP) and replacement of solvents in Europe. Atmospheric Environment 34, 3159–3169.

Arvanitis, T., Nitis, T., Theodoridis, G., Tourlou, P.M., Naneris, C., Moussioupoulos, N., 1997. Synthesis of the 2004 emission inventory. In: Moussioupoulos, N., Papagrigouriou, S. (Eds.), Athens 2004 Air Quality, Athens 2004 Bid Committee, pp. 60–70. Published by EnviroComp Institute, Freemont, California (USA).

Batchvarova, E., Gryning, S.E., 1998. Wind climatology, atmospheric turbulence and internal boundary-layer development in Athens during the medcaphot-trace experiment. Atmospheric Environment 32, 2055–2069.

Bornstein, R.D., Thunis, P., Schayes, G., 1993. Simulation of urban barrier effects on polluted urban boundary layers using the three-dimensional URBMET/TVM model with urban topography—new results from New York City. In: Zannetti, P. (Ed.), Air Pollution. Computational Mechanics Publications, Southampton, Boston, pp. 15–34.

Bougeault, P., Lacarrere, P., 1989. Parameterisation of orography-induced turbulence in a mesobeta-scale model. Monthly Weather Review 117, 1872–1890.

Clappier, A., 1998. A correction method for use in multidimensional time-splitting advection algorithms: application to two- and three-dimensional transport. Monthly Weather Review 126, 232–242.

Clappier, A., Perrochet, P., Martilli, A., Muller, F., Krueger, B.C., 1996. A new non-hydrostatic mesoscale model using a control volume finite element (CVFE) discretisation technique. In: Borrell, P.M., et al. (Ed.), Proceedings of the EUROTRAC Symposium '96. Computational Mechanics Publications, Southampton, pp. 527–553.

Clappier, A., Martilli, A., Grossi, P., Thunis, P., Pasi, F., Krueger, B.C., Calpini, B., Graziani, G., van den Bergh, H., 2000. Effect of sea breeze on air pollution in the Greater Athens Area. Part 1: numerical simulations and field observations. Journal of Applied Meteorology 39, 546–562.

Collella, P., Woodward, P., 1984. The piecewise parabolic method (PPM) for gas dynamical simulations. Journal of Computational Physics 54, 174–201.

Gong, W., Cho, H., 1993. A numerical scheme for the integration of the gas phase chemical rate equations in three-dimensional atmospheric models. Atmospheric Environment 27A, 2147–2160.

Grimmond, C.S.B., Oke, T.R., 2000. Aerodynamic Properties of urban areas derived from analysis of surface form. Journal of Applied Meteorology 38, 1262–1292.

Grimmond, C.S.B., Oke, T.R., 2002. Turbulent heat fluxes in urban areas: observations and a local-scale urban meteorological parameterization scheme (LUMPS). Journal of Applied Meteorology 41, 792–810.

Kallos, G., Kassomenos, P., Pielke, R.A., 1993. Synoptic and mesoscale weather conditions during air pollution episodes in Athens, Greece. Boundary-Layer Meteorology 62, 163–184.

Kastner-Klein, P., Fedorovich, E., Rotach, M.W., 2001. A wind tunnel study of organised and turbulent air motions in urban street canyons. Journal of Wind Engineering and Industrial Aerodynamics 89, 849–861.

Louis, J.F., 1979. A parametric model of vertical eddies fluxes in the atmosphere. Boundary-Layer Meteorology 17, 187–202.

Louka, P., Belcher, S.E., Harrison, R.G., 2000. Coupling between air flow in streets and the well developed boundary layer aloft. Atmospheric Environment 34, 2613–2621.

Madronich, S., 1998. TUV tropospheric ultraviolet and visible radiation model, from the WebSite: http://acd.ucar.edu/models/open/tuv/tuv.html/.

Martilli, A., 2002. Numerical study of urban impact on boundary layer structure: sensitivity to wind speed, urban morphology, and rural soil moisture. Journal of Applied Meteorology 41, 1247–1266.

Martilli, A., Clappier, A., Rotach, M.W., 2002. An urban surface exchange parameterisation for mesoscale models. Boundary-Layer Meteorology 104, 261–304.

Metcalfe, S.E., Whyatt, J.D., Derwent, R.G., O'Donoghue, M., 2002. The regional distribution of ozone across the British Isles and its response to control strategies. Atmospheric Environment 36, 4045–4055.

Moussiopoulos, N., 1994. Air Pollution in Athens Urban Air Pollution, Vol. 1. Computational Mechanics Publications, Boston, MA, pp. 3–41.

Moussiopoulos, N., Sahm, P., Kessler, Ch., 1995. Numerical simulation of photochemical smog formation in Athens, Greece—a case study. Atmospheric Environment 29, 3619–3632.

Moussiopoulos, N., Sahm, P., Karatzas, K., Papalexiou, S., Karagiannidis, A., 1997. Assessing the impact of the new Athens airport to urban air quality with contemporary air pollution models. Atmospheric Environment 31, 1497–1511.

Moussioupoulos, N., Sahm, P., Karatzas, K., Papalexiou, S., Karagiannidis, A., 1997. Assessing the impact of the new Athens Airport to urban air quality with contemporary air pollution models. Atmospheric Environment 31, 1497–1511.

Oke, T.R., 1995. The heat island of the urban boundary layer: characteristics, causes and effects. In: Cermak, J.E., et al. (Ed.), Wind Climate in Cities. Kluwer Academic Publishers, Dordrecht, pp. 81–107.

Palacios, M., Kirchner, F., Martilli, A., Clappier, A., Martin, F., Rodriguez, M.E., 2002. Summer ozone episodes in the Greater Madrid area. Analyzing the Ozone Response to Abatement Strategies by Modelling. Atmospheric Environment 36, 5323–5333.

Ratti, C., Di Sabatino, S., Britte, R., Brown, M., Caton, F., Burian, S., 2001. Analysis of a 3D urban databases with respect to pollution dispersion for a number of European and American cities, Proceedings of the Third International Conference on Urban Air Quality, Loutraki, Greece, 19–23 March, file usm16.pdf in proceedings cdrom (edited by The Institute of Physics, 76 Portland Place, London W1B 1NT).

Rotach, M.W., 1993a. Turbulence close to a rough urban surface. Part 1: Reynolds stress. Boundary-Layer Meteorology 65, 1–28.

Rotach, M.W., 1993b. Turbulence close to a rough urban surface Part 2: variances and gradients. Boundary-Layer Metereology 66, 75–92.

Rotach, M.W., 2001. Simulation of urban-scale dispersion using a lagrangian stochastic dispersion model. Boundary-Layer Meteorology 99, 379–410.

Stockwell, W.R., Kirchner, F., Kuhn, M., Seefeld, S., 1997. A new mechanism for regional atmospheric chemistry modelling. Journal of Geophysical Research 102, 25847–25879.

Tremback, C.J., Kessler, R., 1985. A surface temperature and moisture parameterisation for use in mesoscale numerical models, Proceedings of Seventh conference on Numerical Weather Prediction, Montreal, Quebec, Canada, June 17–20.

Varvayanni, M., Catzaros, N., Konte, J., Staharas, J., Bartzis, J.G., 1998. Development and interaction of thermally driven flows over the Attiki peninsula under northerly background wind—a case study. Atmospheric Environment 32, 2291–2311.

Ziomas, I.C., Coauthors, 1995. A contribution to the study of photochemical smog in the greater Athens Area. Beitr. Phys. Atmos. 68, 191–203.